

Enhanced Photofission- Based, Coincidence/ Multiplicity Inspection Measurements

INMM 2010

James L. Jones
Daren R. Norman
Kevin J. Haskell
Martyn T. Swinhoe
Steve J. Tobin
William H. Geist

July 2010

The INL is a
U.S. Department of Energy
National Laboratory
operated by
Battelle Energy Alliance



This is a preprint of a paper intended for publication in a journal or proceedings. Since changes may be made before publication, this preprint should not be cited or reproduced without permission of the author. This document was prepared as an account of work sponsored by an agency of the United States Government. Neither the United States Government nor any agency thereof, or any of their employees, makes any warranty, expressed or implied, or assumes any legal liability or responsibility for any third party's use, or the results of such use, of any information, apparatus, product or process disclosed in this report, or represents that its use by such third party would not infringe privately owned rights. The views expressed in this paper are not necessarily those of the United States Government or the sponsoring agency.

Enhanced Photofission-based, Coincidence/Multiplicity Inspection Measurements

James L. Jones, Daren R. Norman, Kevin J. Haskell
Idaho National Laboratory
P.O. Box 1625, MS 2802 Idaho Falls, Idaho 83415-2802

Martyn T. Swinhoe, Steve J. Tobin, William H. Geist,
Robert B. Rothrock, and Cory R. Freeman
Los Alamos National Laboratory
P.O. Box 1663, Los Alamos, NM 87545

ABSTRACT

An enhanced active interrogation system has been developed that integrates a transportable Idaho National Laboratory (INL) photonuclear inspection system, using a pulsed bremsstrahlung source and a reconfigurable neutron detection system, with a Los Alamos National Laboratory (LANL) list-mode data acquisition system. A series of active interrogation experiments using various nuclear materials have shown enhanced nuclear material detection and identification utilizing pulsed photofission-induced, neutron coincidence/multiplicity counting between pulses of an electron accelerator operating at energies up to 10 MeV. This paper describes the integrated inspection system and presents some key shielded and unshielded nuclear material inspection results. The enhanced inspection methodology has applicability to homeland security and possible nuclear weapon dismantlement treaties.

*This project has been supported by the US Department of Energy Office of Dismantlement and Transparency under DOE-ID contract number DE-AC07-05ID14517.

INTRODUCTION

Efforts began as early as 2007 in assessing the potential advantages of using a Los Alamos National Laboratory (LANL) list-mode data acquisition system¹ with multiple Idaho National Laboratory (INL) Photonuclear Neutron Detectors (PNDs)² and the INL transportable, selectable-energy (up to a nominal 10 MeV), pulsed linear electron accelerator³ (that is, the Varitron). The objective was to assess time-correlated, photofission delayed neutron measurements between electron accelerator pulses and compare with INL measurements. An initial passive scoping test in August 2007 showed basic feasibility of using the INL PNDs for coincident counting and the potential for enhancing the INL active photonuclear inspection system. The first active test campaign was conducted at INL during April 2008, using a nominal 8-MeV, 125-Hz electron beam operation with $\sim 10 \mu\text{A}$ average beam current. This first campaign focused on the detection of induced delayed neutrons between each 4 μs -wide accelerator pulse. After each accelerator trigger pulse, the data acquisition windows started at 1.9 ms and continued to 7.67 ms for the INL acquisitions and 400 μs to the next accelerator electron pulse for the LANL acquisitions. While higher (up to ~ 10 MeV) nominal energies were possible with this accelerator, the 8-MeV operation was selected for the initial assessment since it represented a typical high-energy radiographic device. A second follow-on test campaign was conducted at INL in May 2009 assessing an enhanced LANL-built, list-mode acquisition system. This second

campaign studied system detection/identification performance utilizing up to nominal 10-MeV electron beam operations, and it provided additional inspection object characterization data. The following sections describe the two active inspection campaigns, their experimental setup, and their results that continue to show overall system feasibility and enhanced inspection performance. The final section provides an overall summary.

EXPERIMENTAL DESCRIPTION AND RESULTS

The INL detection system consists of multiple PNDs (see Figure 1) providing transistor-transistor logic (TTL)-type signals to a Nuclear Data/Canberra 578 Multi-channel Scaler (MCS) module that provides data to a Canberra Genie 2000 acquisition analysis software via a Canberra 556 Acquisition Interface Module (AIM). The system has a data throughput of up to ~500 kHz. A 16-kg PND is 117-cm long with an outer 10.16-cm diameter aluminum housing. The detector contains an internal high-voltage power supply, an INL-built fast preamplifier, and a 10-atm., 2.54-cm diameter, ^3He tube surrounded by concentric rings of polyethylene moderator, cadmium metal, and ~25% boron-loaded, flexible shielding. This physical shielding configuration enables the selective detection of ~0.1-keV to ~2-MeV neutrons, while temporal selectivity enables fission-delayed neutron detection. To help suppress energetic cosmic neutron background contributions, a ~12.5-kg, 15.2-cm wide, 12.7-cm deep, 127-cm tall polyethylene shroud can enclose a PND as shown in Figure 1 (shown without the standard 2.5-cm thick endcaps). For these assessments, the MCS operated with up to eight detector inputs, each with 512, 15- μs wide, temporal channels (with the first channel assigned to be the trigger-counting channel). Hence, the maximum sweep per trigger signal is 7.67 ms (corresponding to the 1/125 Hz, or 8 ms, accelerator operation).



Figure 1. The Photonuclear Neutron Detector (PND) (left) and several PNDs with cosmic background suppression shrouds.

The LANL data acquisition system (see Figure 2) is based on a list-mode module that records the time of arrival of every pulse using up to 32 channels of data. The highest channel is used to

record accelerator trigger pulses. The data are transferred to a personal computer (PC) via an Ethernet connection. The TTL signals from the PND detectors are converted to differential signals on a pair of ribbon cables using a converter box. Both the list-mode module and the converter box require 5V power supplies.

An acquisition program runs on the PC to receive the data packets from the list-mode module. This program stores the data on the PC in a binary file. This file consists of a simple list of pulse arrival times and channels. The data in each file are analyzed by a custom-designed program that allows the user to specify the desired data analysis parameters.

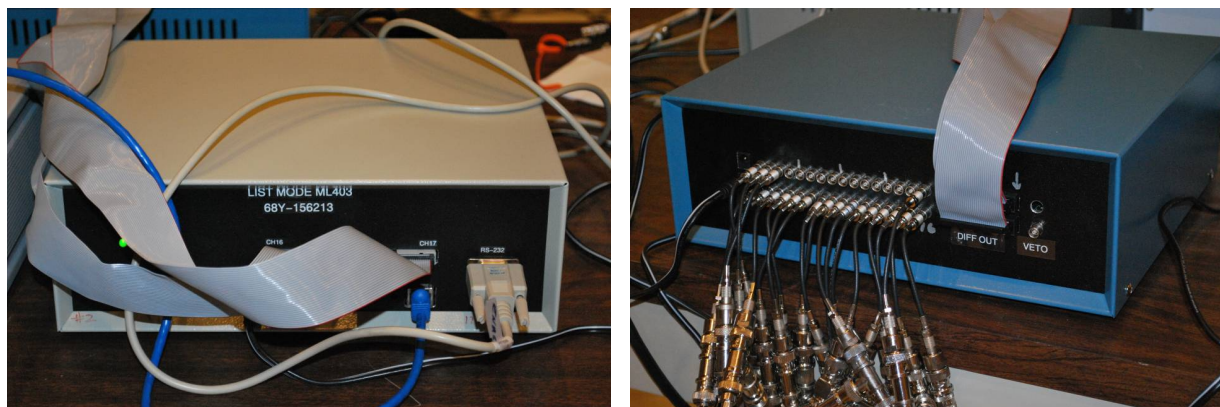


Figure 2. The list-mode data acquisition module (left) and the converter box used to convert TTL signals from the PNDs into a differential signal for the list-mode module.

FIRST ACTIVE CAMPAIGN

Figure 3 shows the experimental configuration of the first campaign using two arrays of 10 vertically-positioned PND detectors (total of 152-cm wide, 13-cm deep, and 127-cm tall) with their polyethylene cosmic radiation suppression shrouds. The arrays are positioned to the left and right of the beam centerline (downstream of the Varitron). All detectors were positioned within two meters forward of the accelerator's bremsstrahlung photon source, and their output signals were connected to the LANL data acquisition system with selected detectors connected to the INL system. An aluminum holder assembly (shown on the pallet between the PNDs) is used for positioning the inspection objects with a laser-aligned, beam centerline. The center two PNDs of each detector bank are located about ~56 cm from the sample location, while the surface of the end-most PNDs (or assembly "edge" detectors) are about 100 cm from the sample locations. For these tests, the Varitron uses a ± 30 degree photon collimator to assure complete irradiation with the nominal 8-MeV bremsstrahlung radiation for any object placed at the defined inspection location.

The specific inspected-object location selected for these tests is the center of an aluminum holder defined by a 20.3-cm tall, 20.3-cm diameter, and 1.3-cm thick holder centered on the beam axis (82-cm from the floor) and having its outer surface located 1 m from the accelerator's photon (bremsstrahlung) source. Hence, a test object placed within the holder configuration will have a nominal 1.1-m source-to-inspection object distance.



Figure 3. Experimental setup of the Varitron accelerator, the multiple PNDs positioned downstream of the accelerator, and the aluminum sample holder between two rows of PNDs.

The main inspection objects assessed in these tests include a non-nuclear material (two stainless-steel plates [$5.1 \times 15.2 \times 0.3$ -cm; 186 g each]) and two nuclear materials (two 93.3% highly enriched uranium (HEU) metal plates [$5.1 \times 10.2 \times 0.3$ -cm: 576 g total] and a single depleted uranium (DU) plate [$10.4 \times 10.4 \times 0.3$ -cm: 605 g]). Each inspection object was assessed with and without a moderator sandwich of polyethylene that consisted of multiple 5.1-cm-square segments 20.3-cm long. To address composite shielding issues (see Figure 4), additional tests included the HEU material sample sandwiched between slabs ($15.2 \times 20.3 \times 2.5$ -cm) of high-Z (i.e., bismuth) shielding and 5.1-cm-square polyethylene segments.



Figure 4. The selected polyethylene and bismuth composite shield configuration. (Nuclear material is sandwiched between slabs of 2.5 cm-thick bismuth and segments of 5.1 cm-square polyethylene.)

An additional assessment included a 55-gallon drum (standard Department of Transportation 6M) filled with 7.9 kg of ^{235}U (unirradiated oxide fuel pins of 46% ^{235}U). The surface of the upright-positioned drum was positioned at one meter from the bremsstrahlung source and centered on the beam centerline axis.

FIRST ACTIVE CAMPAIGN RESULTS

Table 1 presents a summary of the various cases studied in this first experimental assessment using a nominal 8-MeV accelerator operation. In all cases that used nuclear material, the error in the Singles data is less than $\pm 4\%$ and additional data collection time would have been needed to provide a similar error for other data collected (for example, Doubles, Triples, backgrounds). A ^{252}Cf source (5.4×10^4 n/s: based on 540 μCi as of 1/94) was used for system calibration. The list-mode data from two PNDs in the 20-PND configuration were not utilized because of observed signal oscillation problems; hence, the list-mode data acquisition utilized 18 PNDs and considered a larger acquisition window. Double neutron coincident counting was measured.

Some of the acquired MCS and list-mode data are shown in Figure 5 and presented in Table 1. Using the calculated ^{252}Cf source strength and the detector's ^{252}Cf calibration performance of $\sim 3\text{E-}4$ counts/source neutron at one meter (from a prior assessment²), it was estimated that a PND at 1 m should provide at total rate of 16.2 counts/s or about 12.1 counts/s in a 1.9 to 7.67-ms acquisition window between trigger pulses. The right bank edge detector showed 10.8 ± 0.3 counts per second after being corrected for a 0.8 ± 0.08 count/s background. Based on the measurement uncertainties of the physical test configuration used during the source tests, the potential source strength uncertainty, and the estimated calibration performance value, the yield response and the measured response compared well.

Table 1. First test campaign data analysis for a 8-MeV operation (all statistical error within $\pm 4\%$)

Case	Net Singles INL ^a (cts/s)	Singles LANL ^b (cts/s)	Doubles LANL (cts/s)	Doubles/Singles Ratio
^{252}Cf	10.8	367	2.8	0.0076
DU w/o poly	19.0	851	4.9	0.0057
HEU w/o poly	15.7	757	8.7	0.012
DU w/poly	8.8	368	3.3	0.0089
HEU w/poly	17.5	749	35.1	0.047
Poly	0.9	51.3	0.9	0.018
HEU w/Bi & Poly	19.1	787	90.3	0.11
w/Bi & Poly	0.0	174	1.4	0.0079
7.9 kg ^{235}U (DRUM)	128	2614 ^c	243 ^c	0.093 ^c
a. Single PND net counts at one meter from sample location (1.9 to 7.67 ms acquisition window).				
b. Multiple (18) PNDs ≤ 1 m from sample (400 μs to 8 ms acquisition window).				
c. Multiple (18) PNDs ≤ 1 m from sample (3 to 8 ms acquisition window).				

Figure 5 shows that the delayed neutron period starts about 1 ms after the pulse for the small samples and about 3 ms after the accelerator's trigger pulse in the case of the drum (mainly due to the drum's differential die-away). Table 1 results show that the Singles counting rate is a clear indication of the presence of nuclear material (HEU or DU). Note, DU gives more delayed neutrons per gram than ^{235}U and the Singles signal is proportional to the mass (if self-shielding effects are minimal). On the other hand, the Doubles are a clear indication of fissile material rather than just nuclear material. This is true even when the fissile material is shielded with high-Z gamma and/or low-Z neutron shielding.

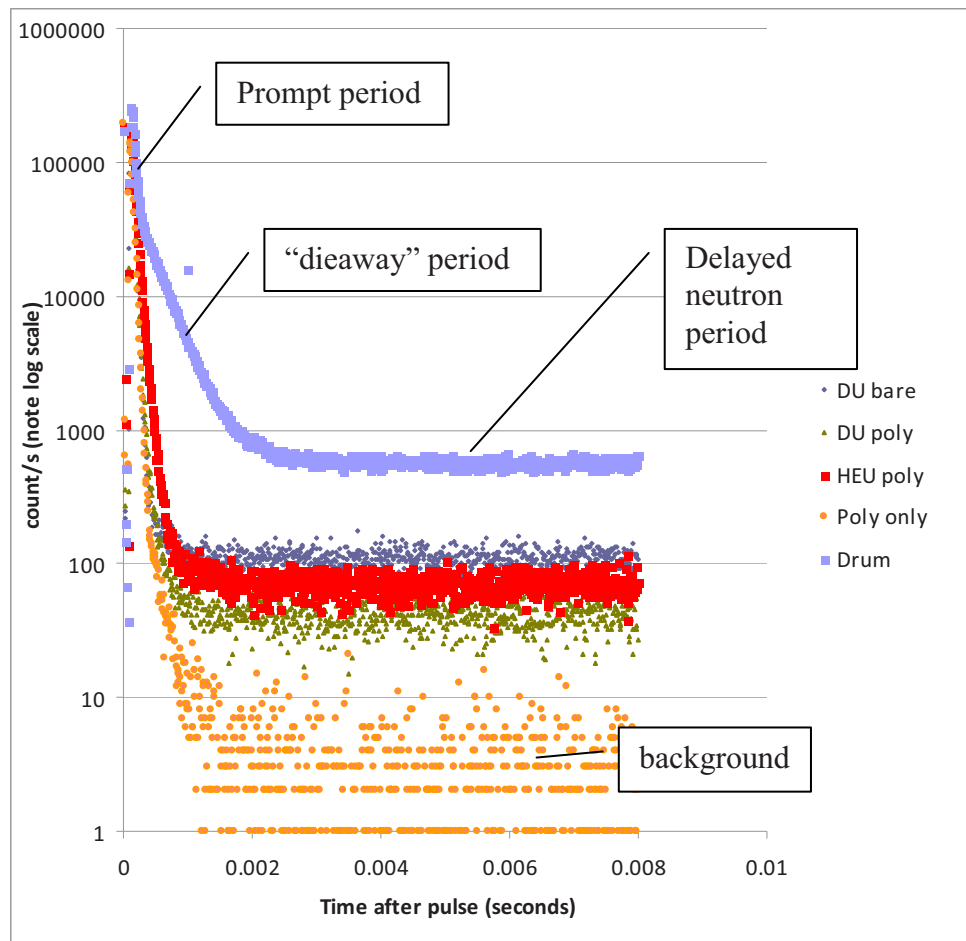


Figure 5. Data for cases collected with list-mode electronics.

The “Poly” case is representative of all non-nuclear material backgrounds. For example, without nuclear material, the total PND single response shows ~ 0.9 counts/s and ~ 0 net counts/s for “Poly” and “w/Bi and Poly” respectively, showing it is essentially independent of the 8-MeV accelerator operation. In general, the single INL detector data and LANL Singles data compare quite well if one realizes that the LANL data are based on an overall 18-PND configuration with each PND located at less than 1 m from the sample locations; whereas the single PND detector used in the INL acquisition corresponded to a 1-m inspected object-to-detector position. The only notable comparison exception is the data for the “w/Bi & Poly” case; which is an artifact of the very low non-nuclear material count rate and its increased relative error for a single detector. In addition, the LANL acquisition window, starting at 400 μ s, includes a small portion of the prompt photoneutron die-away from the photon pulse, which especially affects the comparison when there is a low count rate in the delayed region.

SECOND ACTIVE CAMPAIGN

A second test campaign was performed with a 18-PND detector (with suppression shrouds) configuration that utilizes a narrower detector bank-to-bank separation distance and attempts to

maximize a 4π -type neutron emission detection. This experimental detector configuration is shown in Figure 6 and results with the closest Top, Left, and Right Bank detector distances being 45.5, 37.5, and 37.5 cm, respectively. This test series also focused on electron beam energy dependence while using shielded and unshielded DU and HEU inspection samples having quantities, geometries, and configurations that were almost identical to the first test campaign assessment.



Figure 6. Second test configurations showing the INL Varitron and the detector “house” configuration. (Left, Top, and Right detector banks are defined from the Varitron and looking into the detector “house.”)

SECOND ACTIVE CAMPAIGN RESULTS

The nuclear materials used in these tests were positioned on beam axis at 1.1 m from the photon source. The shielding studied included 5.1-cm polyethylene (see Figure 7) and 2.5-cm thick, 20-cm square bismuth bricks. Using various nominal electron beam energies (i.e., 6, 8, and 10 MeV) and their associated beam currents (that is, 9.5, 10.3, and 3.3 μ s, respectively).

Figure 7 presents representative PND Singles data (for a PND having the closest inspection-to-object distance in the Left Bank) as a function of electron beam energy. Note the Singles data become separated with increasing inspection energy when surrounded with polyethylene shielding but not much separation is seen with bismuth. The separation of the polyethylene data is due to the increased number of thermal fissions in the HEU. The response in the high-Z material is due to attenuation effect on the interrogated photon flux and the negligible effect of neutron slowing down within the bismuth shield. Note the “nil” response without nuclear material within this energy range.

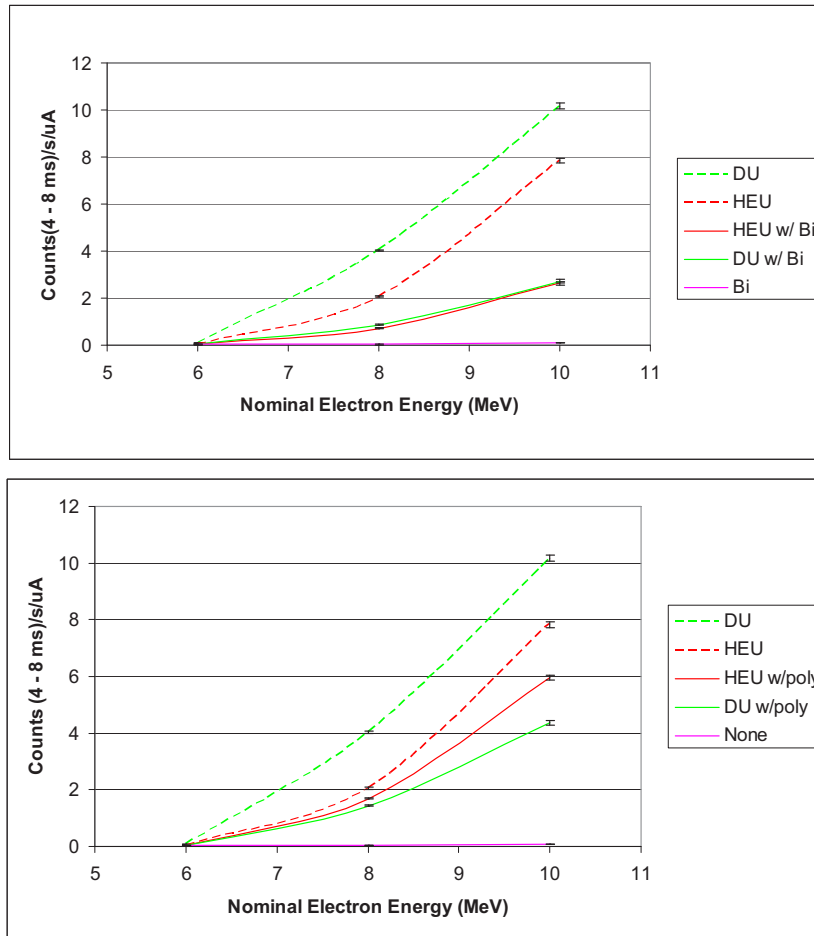


Figure 7. Shielded and unshielded HEU and DU results from the closest PND (Left Bank) for a 4-8-ms acquisition window.

Figure 8-10, shows the corresponding list-mode data: Singles, Doubles and Doubles/Singles ratio, respectively, as a function of electron energy. The Doubles and Doubles/Singles ratio show a clear distinction between those cases with HEU (red) and those without HEU (green).

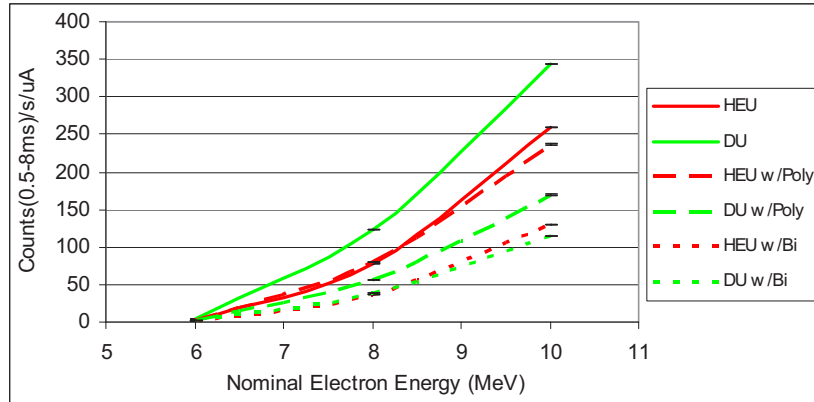


Figure 8. Singles count rates for shielded and unshielded HEU and DU results from list-mode data for a 0.5-8 ms acquisition window.

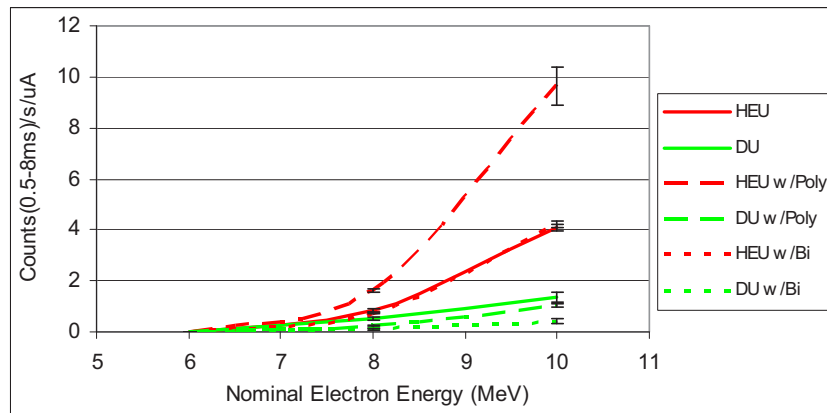


Figure 9. Doubles count rates for shielded and unshielded HEU and DU results from list-mode data for a 0.5-8 ms acquisition window.

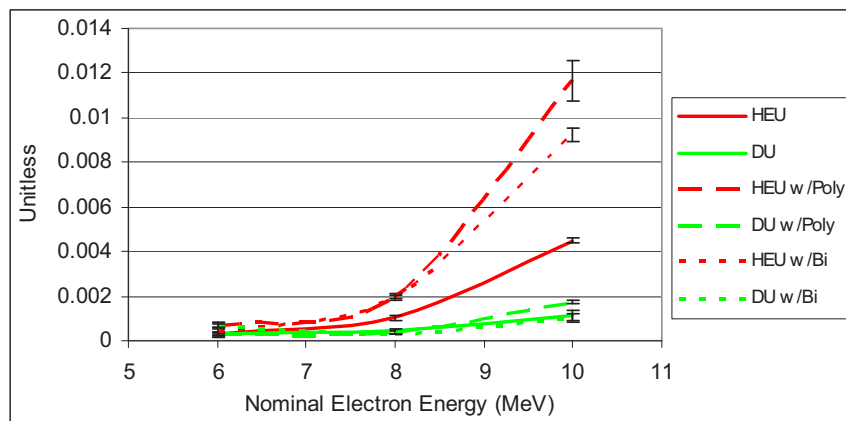


Figure 10. Doubles/Singles ratio for shielded and unshielded HEU and DU results from list-mode data for a 0.5-8 ms acquisition window.

Finally, with the use of radioactive sources (Cf-252 and Pu) and list-mode Single data, Figure 11 shows a potential spatial profiling capability using all detector channels (Right [1-6], Left [7-12] and Top Banks).

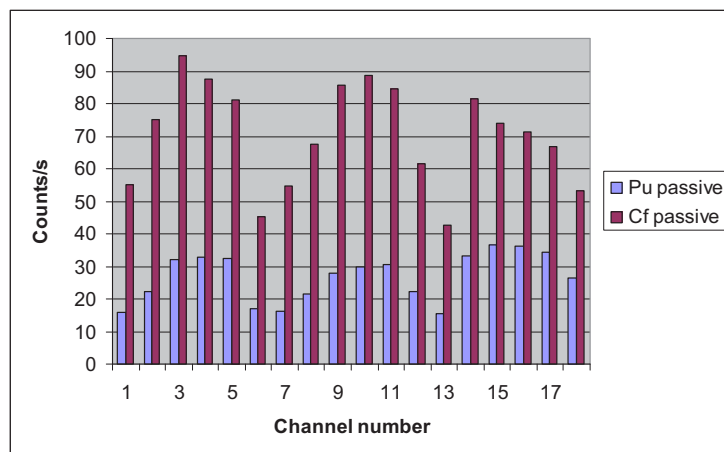


Figure 11. Counting rate for each detector with the Pu and Cf sources.

SUMMARY

This paper presents experimental results supporting the integration of nuclear material detection and identification using an energetic photonuclear-based nuclear material detection method with a photofission-induced, list-mode neutron coincidence counting method between pulses of an electron accelerator. These tests, using up to 10-MeV electron accelerator operations, have demonstrated not only shielded/unshielded nuclear material detection but, more importantly, also appear to indicate a strong ability to enable fissile material identification while essentially being insensitive to non-nuclear materials. The list-mode technique adds additional information, such as the Doubles and spatial profile information, that can be used to identify material types or configurations and appears to be able to see correlated data as soon as $\sim 400 \mu\text{s}$ after each trigger pulse. A prototype data acquisition system and analysis user interface is available. Applications for this inspection method range from supporting various homeland security missions to treaty-related, weapon dismantlement objectives. Future system development work will involve overall system integration and optimization (such as detector configurations and optimal acquisition window between accelerator pulses), improvement to the user interface, evaluating additional composite shield configurations, exploiting the extent of spatial profiling information using the multiple detectors, and assessing accelerator pulse width effects. Finally, some modeling work is suggested to underpin and help optimize the experimental technique.

REFERENCES

1. M. T. Swinhoe, "Experience with List-Mode Data Collection for Safeguards." Los Alamos National Laboratory Report LA-UR-07-1858 April 2007.
2. J. L. Jones, et al., "Photofission-based, Nuclear Material Detection: Technology Demonstration," INEEL Formal Report, INEEL/EXT-02-01406, December 2002.
3. J. L. Jones, et al., "Pulsed Photoneutron Interrogation: The GNT Demonstration System," WINCO Formal Report, WINCO-1225, October 1994.